Thermodynamic Properties of Poly(vinyl alcohol) and Poly(vinyl alcohol–vinyl acetate) Hydrogels

Ferenc Horkay,*,†,‡ Walther Burchard,† Erik Geissler,§ and Anne-Marie Hecht§

Institut für Makromolekulare Chemie, Universität Freiburg, Stefan Meier Strasse 31, D-7800 Freiburg im Breisgau, FRG, Department of Colloid Science, Eötvös Loránd University, Pázmány Péter sétány 2, Pf. 32, H-1518 Budapest, Hungary, and Laboratoire de Spectrométrie Physique (CNRS Associate Laboratory), Université Joseph Fourier de Grenoble, B.P. 87, F-38402 St. Martin d'Hères, France

Received August 17, 1992; Revised Manuscript Received November 27, 1992

ABSTRACT: Osmotic and light scattering observations are reported for chemically cross-linked poly(vinyl alcohol) and poly(vinyl alcohol–vinyl acetate) hydrogels and the corresponding semidilute polymer solutions. The osmotic contribution of the network polymer is obtained from swelling pressure and shear modulus measurements. The free energy of mixing in the cross-linked polymer is found to be significantly smaller than that of the polymer solution at the same concentration. Small-angle neutron scattering and static light scattering measurements indicate the presence of large-scale static structures in the systems. The fluctuating part of the total scattered intensity determined from simultaneous dynamic and static light scattering measurements is compared with the results of macroscopic osmotic observations. Reasonable agreement is found between the results of the two entirely different experiments.

Introduction

The contribution of structural nonuniformities to the equilibrium properties of swollen polymer networks has not been elucidated satisfactorily because of the complexity of the network structures.[1-3] In model elastomers, prepared by end-linking of functionally terminated polymer chains, trapped entanglements, elastically ineffective loops, and pendant chains make the network imperfect. The Flory–Erman constrained junction fluctuation theory assumes that the only effect of topological constraints is the reduction of fluctuations of the junction points.[4,5] Other network theories assume different forms of the constraint contributions.[6,7] The experimental results obtained for end-linked networks are sometimes consistent with existing models.[8-10]

For hydrogels—i.e., water-swollen networks—the situation is in general very complicated as they usually contain more structural imperfections. Hydrogen bonding or association of ionic groups leads to formation of clusters of various sizes and shapes. Although several investigations have been performed on hydrogels, the relationship between the structure and the equilibrium swelling and elastic properties is still not fully understood.

This paper deals with the osmotic and mechanical properties of chemically cross-linked poly(vinyl alcohol) (PVA) and poly(vinyl alcohol–vinyl acetate) (P(VA–VAc)) hydrogels. The polymer chains in aqueous PVA solutions are clustered due to hydrogen bonding.[11,12] It is expected that cluster formation is sterically hindered (i) in PVA networks because cross-links act like large side groups and (ii) in copolymer gels because a certain fraction of hydroxyl groups is replaced by acetate groups. We compare the osmotic properties of aqueous PVA gels with those of PVA solutions and P(VA–VAc) copolymer gels. The acetate content and the statistical copolymer used in the present investigation is 12% (mole/mole). Gels with a nominally identical degree of cross-linking (DC: number of monomer units/number of cross-linker molecules) were synthesized in aqueous solutions of PVA and P(VA–VAc) using glutaraldehyde as cross-linking agent. Here we report the swelling characteristics and the mechanical properties of these networks.

The purpose of this publication is to compare (a) the dependence of the shear modulus and swelling pressure for PVA and P(VA–VAc) hydrogels upon swelling, (b) the thermodynamic polymer–solvent interaction parameters (Flory–Huggins parameter) for the cross-linked polymers and the corresponding polymer solutions, and (c) the results obtained for the longitudinal moduli of the gel from osmotic deswelling and light scattering observations.

Theoretical Section

Thermodynamics of Swollen Polymer Networks. The thermodynamic treatment of a cross-linked polymer is based on the hypothesis that the mixing and elastic components of the solvent chemical potential are additive and separable[13,14]

$$(\Delta\mu_1)_{mix} + (\Delta\mu_1)_{net} = RT \ln a_1 \qquad (1)$$

where $\Delta\mu_1 = \mu_1 - \mu_1^\circ$ (μ_1° is the chemical potential of the pure solvent) and a_1 is the activity of the solvent. The mixing component of the chemical potential is usually assumed to be identical for the cross-linked polymer and the corresponding un-cross-linked polymer solution of infinite molecular weight. According to the Flory–Huggins theory

$$(\Delta\mu_1)_{mix} = RT[\ln(1-\varphi) + (1-P^{-1})\varphi + \chi\varphi^2 + w\varphi^3] \qquad (2)$$

where φ is the volume fraction of the polymer, χ and w are interaction parameters, and P is the degree of polymerization (for a cross-linked polymer $P = \infty$).

Several experimental results indicate that the mixing term in the semidilute regime is described with improved precision by the equation[15]

$$(\Delta\mu_1)_{mix} = A\varphi^n \qquad (3)$$

where $n \approx 2.31$ for good-solvent conditions and $n = 3$ in a Θ diluent.

† Universität Freiburg.
‡ Eötvös Loránd University.
§ Université Joseph Fourier de Grenoble.

0024-9297/93/2226-1296$04.00/0 © 1993 American Chemical Society

The classical James–Guth expression[14,16] yields for the network component of the chemical potential

$$(\Delta\mu_1)_{net} = kT\zeta V_1\varphi^{1/3} \quad (4)$$

where ζ is the cycle rank of the network and V_1 is the partial molar volume of the solvent.

According to a more recent theory due to Flory and Erman,[4,5] the elastic term adopts a complicated form which reduces to eq 4 in the phantom limit. In the affine limit

$$(\Delta\mu_1)_{net} = kT\zeta V_1\varphi^{1/3} - (kT/2)\zeta \ln \varphi^{-1} \quad (5)$$

The second term in eq 5 arises from the contribution of conformational constraints to the elastic free energy. It is assumed that the interchain interactions alter the range of spatial fluctuations of junction points relative to those in a phantom network.

Several alternative expressions have been proposed for the elastic term based on different network models (tube models[17,18] and slip-link model[19,20]).

Aggregation of polymer chains and clustering of junction points have been seen in many real systems.[12,21-23] These nonuniformities are usually specific to the given system and dependent on the condition of preparation. None of the existing theories describes quantitatively the effect of the inhomogeneous distribution of the chains on the elastic and osmotic properties of the swollen network.

Scattering from Polymer Solutions and Gels. At small transfer wave vectors, the intensity of elastically scattered radiation from a neutral polymer solution is inversely proportional to the osmotic compressibility[15]

$$I(Q) = a\frac{kT(\rho_p - \rho_s)^2\varphi^2}{\varphi(\partial\Pi/\partial\varphi)}\frac{1}{1 + Q^2\xi^2} \quad (6)$$

where a is a constant, Q is the scattering wave vector, Π is the osmotic pressure, ξ is the correlation length characterizing the arrangements of the structural elements in the system, and $(\rho_p - \rho_s)^2$ is a constrast factor. In a neutron scattering experiment the contrast factor arises from the difference in the coherent scattering length densities between the polymer and solvent, while in the light scattering experiment it results from differences in the refractive index.

In a gel, because of its finite elasticity, the osmotic pressure should be replaced by the swelling pressure, ω. The scattered intensity is then governed by the longitudinal osmotic modulus

$$M_{os} = \varphi\partial\omega/\partial\varphi + (4/3)G \quad (7)$$

where G is the shear modulus of the swollen network.

In a light scattering experiment the intensity is usually expressed by the Rayleigh ratio

$$R(\theta) = I(\theta)L^2/I_0 \quad (8)$$

where I_0 is the incident light intensity, $I(\theta)$ is the intensity of light scattered at angle θ, and L is the sample–detector distance. The scattered intensity arising from concentration fluctuations in a polymer solution is given by[24]

$$R(\theta) = R(\theta)_{solution} - R(\theta)_{solvent} = RTK\varphi/(\partial\Pi/\partial\varphi) \quad (9)$$

where K is an optical constant. $K = 16\pi^2 n_0^2(\partial n/\partial c)^2/\lambda^4 N_A$, where n_0 is the refractive index of the solvent, $\partial n/\partial c$ is the refractive index increment of the polymer–solvent system, λ is the wavelength of the radiation, and N_A is the Avogadro number.

In gels the total scattered intensity is usually higher than in the corresponding (un-cross-linked) polymer solutions. The excess intensity arises from inhomogeneities of the network structure. The thermodynamics of polymer gels is, however, primarily governed by the freely fluctuating (solution-like) part of the system.[25-28]

Experimental Details

Gel Preparation. Gels were prepared by cross-linking PVA and P(VA–VAc) in aqueous solutions with glutaraldehyde at pH = 1.5 using a method described previously.[29] For the experiments fractionated polymer samples were used (M_W^{PVA} = 110 000, $M_W^{P(VA-Vac)}$ = 128 000). Cross-links were introduced at polymer concentrations c = 3.0, 4.0, 5.0, 5.5, 6.0, 7.0, and 8.0% (w/w); the molar ratio of monomer units to the molecules of cross-linker was 200 at each concentration. At polymer concentrations below 3.0% (w/w) no macroscopic gelation was observed.

The acetate content of the statistical P(VA–VAc) copolymer was 12% (mol/mol).

For the calculation of the polymer volume fractions, φ, the densities of the pure components (ρ_{PVA} = 1.269 g cm^{-3}, $\rho_{P(VA-Vac)}$ = 1.246 g cm^{-3}, and ρ_{water} = 0.9971 g cm^{-3}) were used.

Osmotic and Mechanical Measurements. The water activity in the gels was measured as a function of the polymer concentration using a modified deswelling method.[30] Gels were equilibrated with polymer solutions of known water activity.[31] A semipermeable membrane was inserted between the gel and the solution to prevent the diffusion of the polymer molecules into the swollen network. In the present case poly(vinylpyrrolidone) (M_n = 29 000) was used to adjust the water activity. The measurements were performed in the activity range $0.995 < a_1 < 1.0$. The swelling pressures, ω, of the gels were obtained from the relation

$$\omega = -(RT/V_1)\ln a_1 \quad (10)$$

The additivity of the specific molar volumes of the solvent and the solute in the cross-linked polymer was checked both pycnometrically and optically (by measuring the dimensions of regularly shaped samples at different stages of dilution using a comparator and weighing measurements). In the concentration range $0.02 < \varphi < 0.20$ no systematic deviation from additivity was observed.

The shear modulus measurements were performed on isometric cylindrical gel specimens prepared in a special mold. Swollen networks were uniaxially compressed (at constant volume) between two parallel flat plates. The stress–strain data were determined in the range of deformation ratio $0.7 < \Lambda < 1$. The absence of volume change and barrel distortion was checked by determining the dimensions of the deformed and undeformed gel cylinders. The results were analyzed using the Mooney–Rivlin relation

$$\sigma = C_1(\Lambda - \Lambda^{-2}) + C_2(\Lambda - \Lambda^{-2})/\Lambda^{-1} \quad (11)$$

where σ is the nominal stress (related to the undeformed cross-section of the gel cylinder). The value of C_2 proved to be negligibly small for the gel systems studied. In this situation, the constant C_1 can be identified with the shear modulus of the swollen network.

The viscosities of the polymer solutions were measured using a Haake rotational viscosimeter.

Light Scattering Measurements. The light scattering experiments were performed in the angle range 30–150° using an ALV/SP-86 automatic goniometer (ALV, Langen, Germany) at 25 °C. The light source was a Spectra Physics 2020 krypton ion laser working at a wavelength of λ = 647.1 nm at approximately 300 mW. Intensity correlation functions were measured by an ALV-3000 multibit correlator (ALV, Langen, FRG). In the multisample time mode the correlator contains 192 logarithmically spaced data channels which span nine decades in one measurement. The analysis of the measured autocorrelation function was performed by inverse Laplace transformation using the program CONTIN.[32]

The solution and the gel samples were prepared in Hellma test tubes with an inner diameter of 8 mm. Dust was removed from the homogeneous solutions by filtering them through Teflon filters of 0.45-μm pore size. The sample cell in the goniometer was surrounded by a refractive index matching bath (decalin),

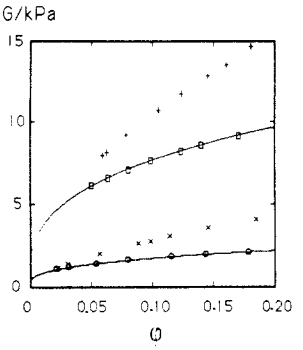

Figure 1. Shear modulus, G, as a function of polymer volume fraction, φ, for PVA and P(VA–VAc) hydrogels. The continuous curves show the theoretical dependence calculated with $m = 1/3$. Symbols: (×) PVA($\varphi = 0.0317$); (+) PVA($\varphi = 0.0639$); (○) P(VA–VAc)($\varphi = 0.0323$); (□) P(VA–VAc)($\varphi = 0.0650$).

which was thermostated by circulating water. For the absolute intensity calibration the scattering from pure toluene was measured.

During the static light scattering measurements the tubes were continuously rotated in the light scattering apparatus to ensure full averaging of the scattered light intensity. In the dynamic measurements the intensity correlation function and the static scattered intensity were determined simultaneously at fixed positions of the sample. For the experimental setup the coherence factor, β, was found to be 0.93 ± 0.02.

Small-Angle Neutron Scattering Measurements. The SANS measurements were performed on the D11 instrument at the Institut Laue-Langevin, Grenoble, using an incident wavelength of 6 Å. The detector was placed at 4 and 16.5 m from the sample. The Q range explored was $0.003 \leq Q \leq 0.25$ Å^{-1}, and counting times of between 20 min and 1 h were used. The ambient temperature during the experiments was 25 ± 1 °C.

Heavy water was used as solvent. The sample cell consisted of 1-mm-thick quartz windows separated by a 1.8-mm-thick Viton O-ring. After radial averaging, corrections for incoherent background, detector response, and cell window scattering were applied.[25] Calibration of the scattered neutron intensity was performed using the signal from a 1-mm-thick water sample in conjunction with the absolute intensity measurements of Ragnetti et al.[33]

Results and Discussion

Osmotic and Mechanical Measurements. In Figure 1 the concentration dependence of the shear modulus is shown for PVA and P(VA–VAc) gels. Inspection of the curves of G vs φ reveals significant differences between the two systems: (i) the shear modulus in the PVA gels increases faster with increasing polymer concentration; (ii) the value of G in the PVA gels is always higher than in the nominally equivalent P(VA–VAc) gels at identical polymer concentration. It is plausible to attribute the observed differences in the shear modulus to the formation of supermolecular structures due to hydrogen bonding of the PVA chains. Physical gelation of PVA solutions is a well-known phenomenon which has been recently investigated by small-angle neutron scattering.[12] In physical gels the size and topology of the clusters usually depend on the polymer concentration in an unpredictable manner. It is reasonable to assume that in lightly cross-linked chemical gels the positions of segments not connected directly to the permanent junctions are not strongly perturbed. Upon deswelling of the gels formation of new contacts between polymer segments is expected, as in physical gelation of polymer solutions. This will result in a monotonic increase in the apparent cross-linking density and hence of the observed elastic modulus.

In P(VA–VAc) gels the formation of physical junctions is sterically hindered by the acetate groups. The presence of 12% (mol/mol) acetate groups significantly reduces the value of G. The concentration dependence of the shear modulus closely follows the theoretical prediction ($G \sim \varphi^{1/3}$).

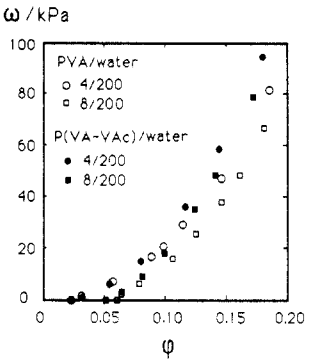

Figure 2. Swelling pressure, ω, as a function of polymer volume fraction, φ, for PVA and P(VA–VAc) hydrogels.

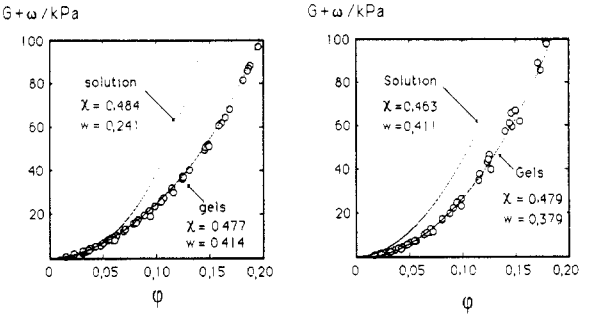

Figure 3. (a, Left) Mixing pressure, $\omega + G$, as a function of polymer volume fraction, φ, for PVA gels. Continuous line refers to the solution of the un-cross-linked polymer of infinite molecular weight. (b, Right) Mixing pressure, $\omega + G$, as a function of polymer volume fraction, φ, for P(VA–VAc) gels. Continuous line refers to the solution of the un-cross-linked polymer of infinite molecular weight.

In Figure 2 the curves of swelling pressure vs polymer volume fraction are shown for the PVA and P(VA–VAc) gels, respectively. It is seen that the dependence of ω on φ for both systems is similar. In the swollen network, the mixing contribution to the swelling pressure can be estimated from the relation

$$\Pi_{mix} = \omega + G \tag{12}$$

where G is known from the mechanical measurements. In Figure 3, both ($\omega + G$) and the osmotic pressure of a solution of the un-cross-linked polymer with infinite molecular weight are plotted as a function of φ. For the PVA/water solution, previously reported data[28] are shown ($\chi = 0.484, w = 0.241$). The osmotic pressure for the P(VA–VAc) solution was calculated from eq 2 using the parameters $\chi = 0.463$ and $w = 0.411$. The deviation between the solution and gel curves is apparent. The parameters χ and w obtained by least-squares fitting of eq 2 through the gel data points are displayed in Figure 3. In both systems the interaction parameters are significantly modified by the presence of cross-links. Similar differences have already been reported for other systems.[29,34–38]

It can also be seen in Figure 3 that for each system the experimental points for the gels lie along the same curve independently of the concentration at which the cross-links were introduced. For these highly swollen gels the systematic dependence of χ upon the cross-linking density, predicted theoretically,[39] cannot be discerned.

Static Light Scattering and Neutron Scattering from PVA Solutions. In Figure 4 $K\varphi/R(\theta)$ is shown as

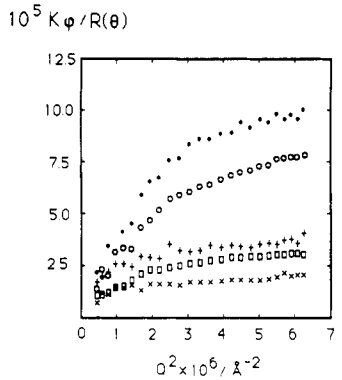

Figure 4. Zimm plots of static light scattering measurements of PVA/water solutions at different concentrations. Symbols: (×) $\varphi = 0.0237$; (□) $\varphi = 0.0397$; (+) $\varphi = 0.0478$; (○) $\varphi = 0.0639$; (●) $\varphi = 0.0803$.

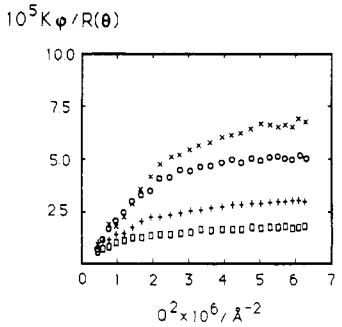

Figure 5. Zimm plots of static light scattering measurements for PVA/water and P(VA-VAc)/water solutions and gels. Symbols: (+) PVA/water solution ($\varphi = 0.0397$); (□) PVA/water gel ($\varphi = 0.0397$); (×) P(VA-VAc)/water solution ($\varphi = 0.0404$); (○) P(VA-VAc)/water gel ($\varphi = 0.0404$).

a function of Q for a set of PVA solutions at different concentrations. For all the solutions the Zimm plots are upward convex. The angular dependence of the scattered intensity in the solutions indicates the presence of nonuniformities of characteristic size comparable to the wavelength of the incident light.

In Figure 5 Zimm plots of PVA and P(VA-VAc) gels are compared with those of the corresponding un-cross-linked solutions. The scattering profiles for the gels and solutions are similar. The solution curves always lie above the gel lines. The linear part of the spectra are steeper for the solutions than for the gels. The scattered intensities from the PVA systems exceed that of the P(VA-VAc)/water systems.

A similar increase in $K\varphi/R(\theta)$ with increasing polymer concentration was reported for several entirely different (polar and nonpolar) polymer–solvent systems in the semidilute regime.[40-43] The observed phenomenon is usually attributed to the presence of inhomogeneities in the solution due to association of the polymer chains. In the case of the PVA/water system, the clustering of PVA molecules in aqueous solutions seems to be responsible for the excess scattered intensity. It was found that heating and then cooling increases $K\varphi/R(\theta)$ as expected for associating solutions. After heating, the $K\varphi/R(\theta)$ vs Q^2 plots were shifted upward but they retained their shape. In a few days the original scattering intensity was recovered. To avoid the uncertainty arising from the time dependence of the scattering intensity, the following standard procedure was used: before the scattering measurements the solutions were heated (95 °C, 3–4 h) and then cooled to 25 °C. In the case of the gels the heat treatment caused practically no change in the measured signal.

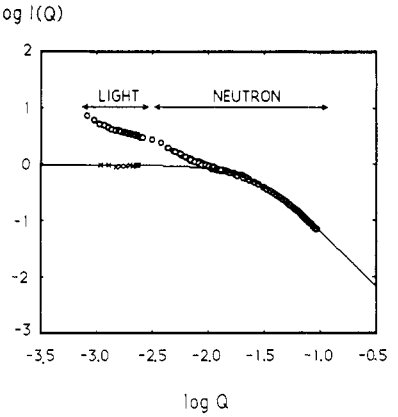

Figure 6. Double-logarithmic plot of the neutron and light scattering intensities, $I(Q)$, as a function of scattering wave vector, Q, for poly(vinyl alcohol) solution at $\varphi = 0.0437$. The continuous line is the Lorentzian fit to the neutron scattering data. The crosses show the intensities, $\langle I_F(Q)\rangle_T$, obtained from the autocorrelation functions. The intensity is in units of cm^{-1}.

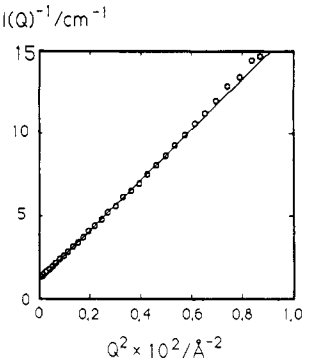

Figure 7. Zimm representation of the neutron scattering data for PVA/water solution at $\varphi = 0.0437$.

In Figure 6 the Q dependence of the normalized light scattering intensity of a PVA solution ($\varphi = 0.0437$) is displayed together with neutron scattering data obtained for the same solution. The Q ranges scanned in the two different experiments almost overlap, resulting in a continuous plot. From the figure the presence of nonuniformities in the PVA solution is visible. The spectrum differs significantly from that of a homogeneous solution (continuous curve), indicating that eq 6 is inadequate to describe the whole scattering curve of the PVA solution. In Figure 7 the same neutron scattering data are shown in a Zimm representation. The linear part of the plot yields for the correlation length $\xi = 38.1$ Å.

The continuous curve in Figure 6 shows the $I(Q)$ vs Q dependence calculated with $\xi = 38.1$ Å. From the intercept at $Q = 0$ the osmotic compressional modulus of the solution is obtained, $K_{os|scatt} = \varphi(\partial\Pi/\partial\varphi) = 12.1$ kPa. This value does not differ significantly from that determined from the concentration dependence of the osmotic pressure, $K_{os|swell} = 14.2$ kPa. (For the calculation of $K_{os|swell}$ the parameters $\chi = 0.484$, $w = 0.241$, and $P = 2400$ were used.)

It can be concluded that the osmotic properties of the PVA solution are governed essentially by ξ. The excess scattered intensity observed at small Q values arises from static nonuniformities that develop in aqueous solution (probably by molecular association through hydrogen bonding). The nonuniformities make no significant contribution to the osmotic properties of the solution.

Quasielastic Light Scattering from PVA and P(VA-VAc) Solutions and Gels. In Figure 8 the intensity–intensity correlation functions are shown for aqueous PVA solutions at 90° at various concentrations.

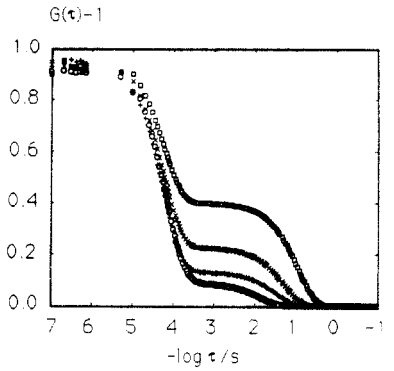

Figure 8. Intensity–intensity correlation functions $G(\tau) - 1$ for PVA/water solutions at 90°. Symbols: (○) $\varphi = 0.0237$; (+) $\varphi = 0.0397$; (×) $\varphi = 0.0478$; (□) $\varphi = 0.0639$.

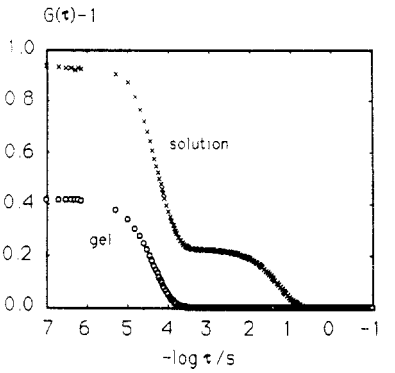

Figure 9. Intensity–intensity correlation function $G(\tau) - 1$ for a PVA/water solution ($\varphi = 0.0478$) and the corresponding hydrogel measured at $\theta = 90°$.

Two relaxation processes can be clearly distinguished, differing by approximately 3 orders of magnitude. The fast part of the relaxation spectrum can be identified with the cooperative motion of the entangled solution (gel-like mode). It is sometimes assumed[44] that the slow part reflects center-of-mass diffusion of clusters. This behavior is in qualitative agreement with the results of the static scattering experiments.

In Figure 9 the correlation function of a PVA gel ($\varphi = 0.0437$) measured at $\theta = 90°$ is shown together with that of the corresponding solution. There are distinct differences between the solution and the gel curves: in the gel the initial amplitude of the correlation function is decreased and the slow mode relaxation is absent.

A study of the relaxational behavior of aqueous PVA solutions and gels prepared according to the procedure developed by us has been reported recently by Fang and Brown.[44] Here we focus primarily on the thermodynamic information obtained from complementary osmotic and scattering measurements.

Analysis of the correlation function allows the determination of the osmotic compressional modulus. For a solution of freely diffusing particles the normalized intensity–intensity correlation function (homodyne signal) is given by

$$G(Q,\tau) = 1 + \beta[g(Q,\tau)]^2 \qquad (13)$$

where $g(Q,\tau)$ is the normalized field correlation function and β is the coherence factor ($\beta \leq 1$).

In a system containing large-scale, stationary nonuniformities which act as local oscillators the detection mode is no longer homodyne. The resulting heterodyned intensity correlation function is given by[45-47]

$$G(Q,\tau) = 1 + \beta[2X(1-X)g(Q,\tau) + X^2 g(Q,\tau)^2] \qquad (14)$$

where τ is the delay time and $X = \langle I_F(Q)\rangle_T / \langle I(Q)\rangle_T$. Here, $\langle I_F(Q)\rangle_T$ is the time-averaged intensity of the fluctuating component and $\langle I(Q)\rangle_T$ is the total scattered intensity.

In the PVA and P(VA–VAc) solutions and gels the presence of large-scale structural nonuniformities detected by static light and neutron scattering heterodyne the light scattered by the fluctuating part of the system. Consequently, the correlation function should be analyzed by eq 14. At the zero-time limit, eq 14 yields

$$X = 1 - [1 + \beta - G(Q,0)]^{1/2}/\beta^{1/2} \qquad (15)$$

where $G(Q,0)$ is the initial amplitude (at $\tau = 0$) of the intensity–intensity correlation function.

In Figure 10 the fluctuating component of the total scattered intensity, $\langle I_F(Q)\rangle_T = \langle R(\theta)/K\varphi\rangle_F$, is shown as a function of Q^2 for PVA solution and gel samples. It can be seen that $\langle I_F(Q)\rangle_T$ is practically independent of Q within the limits of the experimental uncertainty.

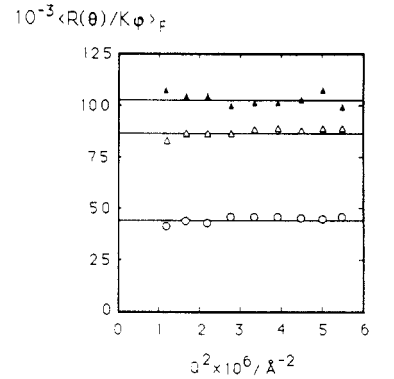

Figure 10. Fluctuating part of the total scattered intensity, $\langle I_F(Q)\rangle_T = \langle R(\theta)/K\varphi\rangle_F$, as a function of Q^2 for PVA solution and gel samples. Symbols: (○) PVA/water solution ($\varphi = 0.0803$); (△) PVA/water solution ($\varphi = 0.0437$); (▲) PVA/water gel ($\varphi = 0.0437$).

The $\langle I_F(Q)\rangle_T$ values obtained from the correlation functions are denoted by crosses in Figure 6. These points lie on the horizontal part of the theoretical (Lorentzian) curve calculated by eq 6 using the value of ξ (=38.1 Å) determined from the neutron scattering data displayed in Figure 7. The agreement between the light and the neutron scattering results is satisfactory.

Quasielastic light scattering measurements yield another structure-sensitive parameter: the hydrodynamic correlation length, ξ_h. From the normalized intensity autocorrelation function, $G(Q,\tau)$, with the assumption of homodyne conditions, an apparent diffusion coefficient (D_{app}) is obtained,

$$\ln[G(Q,\tau) - 1] = \ln(\beta) - 2D_{app}Q^2 t + \ldots \qquad (16)$$

The relation between D_{app} and the cooperative diffusion coefficient, D_c, which describes the collective motions of the chains and hence the swelling of the whole gel,[48-50] is simply

$$D_c = (2 - X)D_{app} \qquad (17)$$

Note that when account is taken of solvent backflow and the symmetry of the kinetic coefficients, we have[51]

$$D_c = (2 - X)D_{app}/(1 - \varphi)^2 \qquad (17a)$$

For the concentration range explored here, however, this modification is of marginal significance.

Under conditions of strong heterodyning, $X \ll 1$, yielding $D_c \approx 2D_{app}$. In this case the factor 2 disappears in eq 16.

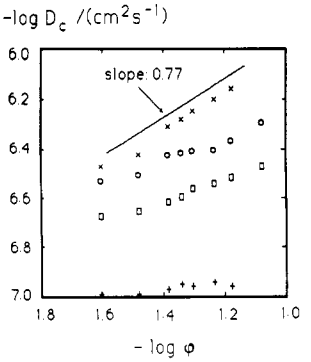

Figure 11. Double-logarithmic plot of the diffusion coefficients, D_c and D^*, as a function of polymer volume fraction, φ, for PVA/water solutions and PVA hydrogels measured at $\theta = 90°$. D_c was obtained by eq 17 ((○) solutions; (×) gels) and D^* by eq 20 ((□) solutions; (+) gels).

Using the Stokes–Einstein relation, the hydrodynamic correlation length is obtained

$$\xi_h = kT/6\pi\eta D_c \tag{18}$$

where η is the viscosity of the solvent.

In Figure 11 the concentration dependence of the diffusion coefficient of the fast relaxation mode is shown for PVA gels and solutions at $\theta = 90°$. The values obtained for D_c using the CONTIN routine were in reasonable agreement with those determined by the cumulant method, assuming partial heterodyning. Similar agreement was also found by assuming that $g(Q,\tau)$ in the gels exhibits a single relaxation process, while that of the solutions contains only two well-resolved processes. It can be seen in the figure that the values of D_c for the gels exceed those of the solutions. The continuous line shows the theoretical slopes of 0.77 in good-solvent conditions. It is noteworthy that the interaction parameters for the PVA/water solutions displayed in Figure 3a are closer to the values expected for a Θ system.

Recent theoretical considerations due to Pusey et al.[47,52,53] allow an alternative treatment of the dynamic light scattering data. According to this theory, the ensemble-average correlation function of a nonergodic medium can be obtained from the measurements of the time-average correlation function at a given location in the sample and the ensemble-average total intensity, $\langle I(Q)\rangle_E$. The ensemble-average field correlation function is then given as

$$g_E(Q,\tau) = (Y-1)/Y + [G(Q,\tau) - G(Q,0) + 1]^{1/2}/Y \tag{19}$$

where $Y = \langle I(Q)\rangle_E/\langle I(Q)\rangle_T$. Equation 19 yields the same intensity for the fluctuating component as that obtained by using eq 14 in conjunction with eq 15. Furthermore, Joosten et al.[52] introduce a new diffusion coefficient, denoted here by D^*:

$$D^* = D_{app}[G(Q,0) - 1]/Y \tag{20}$$

The values of D^* calculated by eq 20, also displayed in Figure 11, are far smaller than D_c obtained from eq 17. Measurements by independent techniques[48-50] have, however, established that D_c is the diffusion coefficient that controls the macroscopic rate of swelling in gels. Since D^* possesses no corresponding macroscopic role, its physical meaning is difficult to situate.

Equations 16 and 17 allow the determination of the slow-mode diffusion coefficient, D_{slow}, for the solutions. Owing to the slow continuous structural changes occurring in these solutions, especially at higher concentration, the precision in the measurement of the slow relaxation is poorer, and we cannot state unambiguously from the Q dependence that this process is purely diffusive. It is, however, clear that D_{slow} is predominantly a mutual diffusion coefficient in the viscous medium. The main results of this analysis are summarized in Table I (third and fifth columns).

Table I
Diffusion Coefficients and the Size of the Associations in PVA/Water Solutions

φ	$10^7 D_c$ (cm^2 s^{-1})	$10^{10} D_{slow}$ (cm^2 s^{-1})	η (P)	$R_h{}^a$ (Å)	d^b (Å)	X^c
0.0237	2.94	10.8	0.153	1320	325	0.70
0.0317	3.10	6.2	0.245	1434	343	0.66
0.0478	3.82	3.6	0.403	1506	366	0.52
0.0639	4.10	1.9	0.687	1671	410	0.37
0.0803	4.86	0.5	2.209	1976	458	0.31

[a] Calculated from D_{slow} using eq 18. For the calculation the viscosity of the polymer solution was used. The results are obtained at scattering angle $\theta = 90°$. [b] Calculated from static light scattering data using eq 21. [c] For fully fluctuating solutions, with two relaxation modes, this ratio refers to the relative intensity of the fast relaxation process.

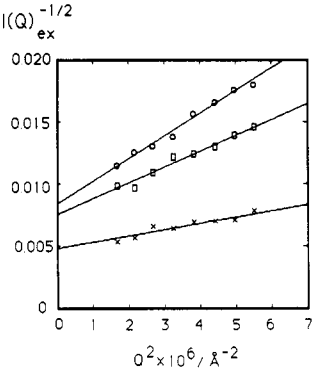

Figure 12. Debye–Bueche plot of excess scattered intensity for PVA/water solutions. Symbols: (×) $\varphi = 0.0237$; (□) $\varphi = 0.0639$; (○) $\varphi = 0.0803$.

Static light scattering provides an independent estimate of the radius of gyration of the associations, R_g. According to the Debye–Bueche theory,[54-56] the excess scattered intensity, $I(Q)_{ex}$ (=$\langle R(\theta)/K\varphi\rangle - \langle I_F(Q)\rangle_T$), arising from long-range nonuniformities of the system is given by

$$I(Q)_{ex} = Kb^2d^3/(1 + d^2Q^2)^{-2} \tag{21}$$

where d is the characteristic size of the inhomogeneities and b^2 is the mean square fluctuation of the refractive index.

In Figure 12 typical plots of $I(Q)_{ex}^{-1/2}$ vs Q^2 are shown for PVA/water solutions. The values obtained for the parameter d from the slopes of the resulting straight lines are displayed in the sixth column of Table I. The apparent radius of gyration of the associations is obtained from the relation $R_g = (6d)^{1/2}$. The ratio of R_g/R_h (R_h is the hydrodynamic correlation length calculated from D_{slow}) is approximately independent of the polymer concentration if in the Stokes–Einstein relationship the actual viscosity of the PVA solution is used. The value of this ratio (≈0.6) is close to that of a sphere. It should, however, be emphasized that the replacement of the solvent viscosity by that of the solution in eq 18 is a bold approximation and only applies in the case where the concentration of the slowly moving particles is small.

Information on the structural changes due to cross-linking can be found from Figure 13, where the scattered intensities $\langle I_F(Q)\rangle_T$ of the PVA gels are compared with those of the corresponding solutions. Inspection of the experimental data at low polymer concentration ($\varphi < 0.048$)

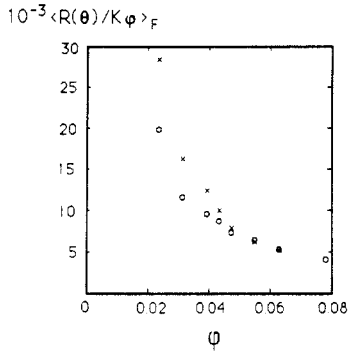

Figure 13. Fluctuating part of the total scattered intensity, $\langle R(\theta)/K\varphi\rangle_F$, as a function of the polymer volume fraction, φ, for PVA/water solutions (○) and gels (×).

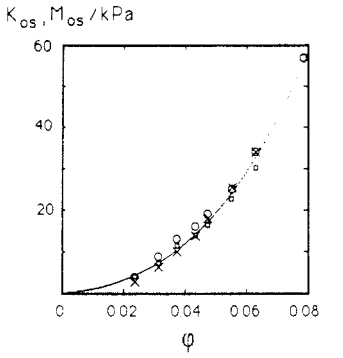

Figure 14. Comparison between measured and calculated values of K_{os} and M_{os} for PVA/water solutions and gels, respectively. (○) K_{os} obtained from light scattering observations. The continuous curve shows the variation of K_{os} for the polymer solution calculated with the parameters $\chi = 0.484$ and $w = 0.241$. (□) $M_{os} = \varphi\partial\omega/\partial\varphi + 4G/3$ calculated from swelling pressure and shear modulus measurements. Crosses denote M_{os} obtained from light scattering data.

reveals excess scattered intensity in the gels. The deviation between the cross-linked and un-cross-linked systems decreases with increasing polymer concentration. Above $\varphi = 0.048$ the scattered intensities from the gels and the corresponding solutions are practically identical. This finding is in agreement with the results reported by Joosten et al.[53]

The higher scattered intensities from the gels at low polymer concentration are consistent with the macroscopic osmotic observations. The osmotic compressional modulus of the polymer–solvent system is usually reduced by cross-linking.[35,37] This reduction is not compensated by the small shear moduli of the lightly cross-linked PVA gels prepared at low polymer concentration.

In Figure 14 the compressional osmotic moduli of PVA solutions, K_{os}, and the longitudinal osmotic moduli of the PVA hydrogels, M_{os}, obtained from light scattering observations are compared with the corresponding quantities determined from macroscopic osmotic measurements. The continuous line in the figure was calculated by eq 22

$$K_{os} = \frac{RT}{V_1}\left[\frac{\varphi}{1-\varphi} - \left(1 - \frac{1}{P}\right)\varphi - 2\chi\varphi^2 - 3w\varphi^3\right] \quad (22)$$

using the parameters χ and w displayed in Figure 3a. The figure shows that at low polymer concentration M_{os} obtained from the light scattering data is smaller than K_{os}. The difference between the two moduli decreases with increasing polymer concentration. It can also be seen that there is no systematic deviation between the results obtained by the osmotic and the light scattering measurements.

Conclusions

The mechanical properties of PVA hydrogels are significantly different from those of nominally equivalent P(VA–VAc) copolymer gels. In the P(VA–VAc) gels the shear modulus closely follows the concentration dependence predicted by rubber elasticity theory. In the PVA gels G increases faster with the polymer concentration.

The osmotic contribution of the network polymer determined from swelling pressure and shear modulus data is smaller than the osmotic pressure of the corresponding polymer solution (at identical concentration).

The results of small-angle neutron scattering and static light scattering measurements indicate the presence of large-scale static nonuniformities in both the solutions and the gels. These nonuniformities make no significant contribution to the thermodynamic properties.

The experimental values obtained for the compressional modulus and the longitudinal osmotic modulus from the fluctuating part of the total scattered intensity are in agreement with the results of independent osmotic and mechanical measurements.

At lower polymer concentration ($\varphi < 0.048$) the fluctuating component of the scattered intensity from the gel significantly exceeds that of the solution. This finding is consistent with the results of the macroscopic osmotic observations; i.e., the osmotic compressional modulus is strongly reduced by cross-linking. The reduction of K_{os} is not compensated by the small value of the shear modulus in the lightly cross-linked PVA gels.

Acknowledgment. F.H. acknowledges a research fellowship from the Alexander von Humboldt Stiftung. We are grateful to the Institut Laue–Langevin for beam time on the D11 instrument. This work is part of a joint CNRS–Hungarian Academy of Sciences project. We also acknowledge research Contract OTKA No. 2158 from the Hungarian Academy of Sciences.

References and Notes

(1) Eichinger, B. E. *Annu. Rev. Phys. Chem.* **1983**, *34*, 359.
(2) Gottlieb, M.; Gaylord, R. J. *Macromolecules* **1984**, *17*, 2024.
(3) Queslel, P. J.; Mark, J. E. *Adv. Polym. Sci.* **1985**, *71*, 229.
(4) Flory, P. J. *J. Chem. Phys.* **1977**, *60*, 5720.
(5) Flory, P. J.; Erman, B. *Macromolecules* **1982**, *15*, 800.
(6) Marrucci, G. *Macromolecules* **1981**, *14*, 434.
(7) Graessley, W. W. *Adv. Polym. Sci.* **1982**, *47*, 67.
(8) Mark, J. E. *Adv. Polym. Sci.* **1981**, *44*, 1.
(9) Erman, B.; Flory, P. J. *Macromolecules* **1982**, *15*, 806.
(10) Queslel, P. J.; Mark, J. E. *J. Polym. Sci., Polym. Phys. Ed.* **1984**, *22*, 1201.
(11) Komatsu, M.; Inoue, T.; Miyasaka, K. *J. Polym. Sci., Polym. Phys. Ed.* **1986**, *24*, 303.
(12) Wu, W.; Shibayama, M.; Roy, S.; Kurokawa, H.; Coyne, L. D.; Nomura, S.; Stein, R. S. *Macromolecules* **1990**, *23*, 2245.
(13) Flory, P. J. *Principles of Polymer Chemistry*; Cornell University Press: Ithaca, NY, 1953.
(14) Treloar, L. R. G. *The Physics of Rubber Elasticity*, 3rd ed.; Clarendon: Oxford, 1975.
(15) de Gennes, P.-G. *Scaling Concepts in Polymer Physics*; Cornell University Press: Ithaca, NY, 1979.
(16) James, H. M.; Guth, E. J. *J. Chem. Phys.* **1943**, *11*, 455.
(17) Edwards, S. F. *Proc. Phys. Soc.* **1967**, *92*, 9.
(18) Di Marzio, E. A. *Polym. Prepr. (Am. Chem. Soc., Div. Polym. Chem.)* **1986**, *9*, 256.
(19) Marrucci, G. *Rheol. Acta* **1979**, *18*, 193.
(20) Ball, R. C.; Doi, M.; Edwards, S. F.; Warner, M. *Polymer* **1981**, *22*, 1010.
(21) Wun, K. L.; Prins, W. *J. Polym. Sci., Polym. Phys. Ed.* **1974**, *12*, 533.
(22) Hecht, A.-M.; Duplessix, R.; Geissler, E. *Macromolecules* **1985**, *18*, 2167.
(23) Tan, H.-M.; Moet, A.; Hiltner, A.; Baer, E. *Macromolecules* **1983**, *16*, 28.

(24) Kerker, M. *The Scattering of Light*; Academic Press: New York, 1969.
(25) Mallam, S.; Horkay, F.; Hecht, A.-M.; Rennie, A. R.; Geissler, E. *Macromolecules* **1991**, *23*, 543.
(26) Horkay, F.; Hecht, A.-M.; Mallam, S.; Geissler, E.; Rennie, A. R. *Macromolecules* **1991**, *24*, 2896.
(27) Hecht, A.-M.; Horkay, F.; Geissler, E.; Benoit, J. P. *Macromolecules* **1991**, *24*, 4183.
(28) Geissler, E.; Horkay, F.; Hecht, A.-M. *Macromolecules* **1991**, *24*, 6006.
(29) Horkay, F.; Zrínyi, M. *Macromolecules* **1982**, *15*, 1306.
(30) Nagy, M.; Horkay, F. *Acta Chim. Acad. Sci. Hung.* **1980**, *104*, 49.
(31) Vink, H. *Eur. Polym. J.* **1971**, *7*, 1411.
(32) Provencher, S. W. CONTIN (Version 2), Göttingen, 1984.
(33) Ragnetti, M.; Geiser, D.; Höcker, H.; Oberthür, R. C. *Makromol. Chem.* **1985**, *186*, 1701.
(34) McKenna, G. B.; Flynn, K. M.; Chen, Y. *Polym. Commun.* **1988**, *29*, 272.
(35) Horkay, F.; Hecht, A.-M.; Geissler, E. *Macromolecules* **1989**, *22*, 2007.
(36) McKenna, G. B.; Flynn, K. M.; Chen, Y. *Macromolecules* **1989**, *22*, 4507.
(37) Horkay, F.; Hecht, A.-M.; Geissler, E. *J. Chem. Phys.* **1989**, *91*, 2706.
(38) McKenna, G. B.; Flynn, K. M.; Chen, Y. *Polymer* **1990**, *31*, 1937.
(39) Freed, K. F.; Pesci, A. I. *Macromolecules* **1989**, *22*, 4048.
(40) Koberstein, J. T.; Picot, C.; Benoit, H. *Polymer* **1985**, *26*, 641.
(41) Guenet, J. M.; Willmoth, N. F. F.; Ellsmore, P. A. *Polym. Commun.* **1983**, *24*, 30.
(42) Gan, J. Y. S.; Francois, J.; Guenet, J. M. *Macromolecules* **1986**, *19*, 173.
(43) Hara, M.; Nakajima, A. *Polym. J. Jpn.* **1980**, *12*, 101.
(44) Fang, L.; Brown, W. *Macromolecules* **1990**, *23*, 3284.
(45) Sellen, D. B. *J. Polym. Sci., Polym. Phys. Ed.* **1987**, *25*, 699.
(46) Geissler, E. In *Dynamic Light Scattering, The Method and Some Applications*; Brown, W., Ed.; Oxford University Press, in press.
(47) Pusey, P. N.; van Megen, W. *Physica A* **1989**, *157*, 705.
(48) Tanaka, T.; Fillmore, D. J. *J. Chem. Phys.* **1979**, *70*, 1214.
(49) Geissler, E.; Hecht, A.-M. *J. Chem. Phys.* **1982**, *77*, 1548.
(50) Peters, A.; Candau, S. J. *Macromolecules* **1986**, *19*, 1952; **1988**, *21*, 2278.
(51) Vink, H. *J. Chem. Soc., Faraday Trans.* **1985**, *81*, 1725.
(52) Joosten, J. G. H.; Geladé, E. T. F.; Pusey, P. N. *Phys. Rev. A* **1990**, *42*, 2161.
(53) Joosten, J. G. H.; McCarthy, J. L.; Pusey, P. N. *Macromolecules* **1991**, *24*, 6690.
(54) Debye, P. *J. Chem. Phys.* **1959**, *31*, 680.
(55) Bueche, F. *J. Colloid Interface Sci.* **1970**, *33*, 61.
(56) Stein, R. S. *J. Polym. Sci., Polym. Phys. Ed.* **1969**, *7*, 657.